Comparison of dimensional accuracies of stereolithography and powder binder printing

Abstract

This paper presents a comparative experimental investigation of the dimensional accuracies of two widely used rapid prototyping (RP) processes: stereolithography (SLA) and powder binder printing (PBP). Four replicates of a purpose-designed component using each RP process were fabricated, and the measurements of the internal and external features of all surfaces were performed using a general-purpose coordinate measurement machine. The results showed that in both cases, the main cause of dimensional variations was the volumetric change inherent in the process. The precision of SLA was far better than that of PBP. The dimensional accuracy of SLA was better in the z direction, whereas PBP produced better dimensional accuracy in the x-y plane. In both RP processes, the height error consisted of two components: constant error and cumulative error. The constant error component was equal to the datum surface error. SLA yielded an average datum surface error that was 68% higher than in PBP. The height error of SLA improved with the increase in nominal height, whereas it deteriorated in PBP.

Keywords *– 3D printing, stereolithography, powder binder printing, rapid prototyping, dimensional error*

1. Introduction

The emerging field of three-dimensional (3D) printing has much potential in the contemporary world of commercial manufacturing largely because of its inherent flexibility. 3D printing uses data from CAD files to create a 3D object through an automated layer-by-layer manufacturing process. In today's rapidly changing consumer preferences and accelerating technological development, flexible manufacturing is desirable from the perspectives of both production and consumer sales. Since the development of the stereolithography (SLA) process in 1987, numerous alternate 3D printing processes have used different methods and materials to create 3D objects [1]. Other commonly used 3D printing processes are selective laser sintering (SLS), fused deposition modelling (FDM), powder binder printing (PBP), and electron beam additive manufacturing (EBAM). According to Kruth et al. [2], the poor dimensional control of these processes was a major limitation that prevented their further penetration into the manufacturing industry.

This paper presents a comparative experimental investigation of the dimensional accuracies of two widely used rapid prototyping (RP) processes: SLA and PBP. Sub-sections 1.1 and 1.2 below briefly introduce the SLA and PBP processes and review the available literature on their dimensional accuracy.

1.1 Stereolithography

Developed in the 1980s by Charles Hull of 3D Systems Inc., SLA was the first commercial RP machine of its kind [3]. SLA fabricates 3D objects by photo-curing a liquid resin using an ultraviolet (UV) laser in a layer-by-layer approach. An SLA machine consists of a horizontal platform supported by a vertical piston that is

submerged in a vat filled with photo-curable liquid. The platform begins the process at a position below the surface of the liquid and it is set at a depth equal to the thickness of one layer. A laser then scans the surface in a predetermined manner, creating solid material where needed in the x-y plane. This is achieved through the use of a controlled optical scanning system that directs the laser using a pivoting mirror. Once the first layer of the unfinished part is complete, the platform is lowered until the top surface of the part is submerged in the liquid at a depth equal to the thickness of the new layer to be created. Due to the nature of this process, each individual layer is selectively traced out by outlining the borders of the object being built. Hatching or weaving patterns are then projected onto the area depending on the selected hatching styles. This results in a 'honeycomb' interior in which the spaces are filled with liquid resin and then encapsulated in a solid skin on both the upper and lower surfaces. The hatch or build style applied promotes the gelling and solidification of the cross-sections [4]. A blade helps to spread the viscous resin over the surface of the previous layer in order to create the next layer. The process is repeated until the part is complete, with each layer bonding to the previous layer. After being scanned by the UV laser, the part is about 95% cured [5]. The post-curing process, which is often performed in a UV chamber or thermal oven, is required to complete the solidification process and improve the mechanical properties of the object.

The major cause of errors during the SLA process is the volumetric shrinkage of resin during photo-polymerisation. Two types of shrinkage stemming from the photopolymer reaction occur during the SLA process. The first is caused by the formation of the polymer bond. As the pre-polymer liquid state is less dense than the solid polymer state, the volume of the solid polymer formed is less than the volume of pre-polymer liquid

from which it was formed. The second cause of shrinkage is the thermal effect, which results from the exothermic chemical reaction during photo-polymerisation. This thermal effect results in an instantaneous rise in temperature that causes the photopolymer to expand upon formation. Simultaneously, heat is lost to the surroundings, which causes the solid to shrink. The combination of these two forms of shrinkage is known to result in non-uniform internal stresses that lead to the warping of the components [6].

Size and shape variations in the laser beam represent another cause of errors during the SLA process. The input command for the laser system is to create lines of zero width, although the laser beam itself has a finite width. Therefore, software compensation is necessary to account for the laser beam's width. Most of the embedded software in RP systems considers the beam diameter to be constant. However, the beam diameter actually varies in size and shape in the x-y plane due to the angle the beam makes with respect to the centreline of the vat. As the laser beam moves to the outer edges of the platform, the beam produces an elliptical spot on the surface of the resin with a major diameter larger than the nominal beam diameter [7]. Bjørke [8] and his research group performed a simulated SLA experiment by placing a piece of UV sensitive photographic paper at the same level as the resin and using the same laser delivery system. They reported that 50% of the dimensional error measured on the completed part already existed on the photographic paper prior to any volumetric change in the material. Moreover, the beam cures the resin at the centre of the platform in a straight line, whereas at the edges the beam deviates from the vertical plane, which affects the shape of the final part [7].

Narahara et al. [9] examined the effects of the reaction-related heat on both the initial linear shrinkage and deformation of parts produced using SLA. They concluded that the variation in linear shrinkage was directly proportional to the decrease in temperature after the initial photo-polymerisation reaction occurred. Salmoria et al. [10] evaluated the impact of post-curing and laser-manufacturing parameters on the properties of the photosensitive resin used in SLA and found that the variation in linear dimensional behaviour depends on the degree of cure influenced by the laser's power, the resin's photosensitivity characteristics and other manufacturing parameters. Huang et al. [11] reported that curling was most prominent on the bottom of the part closest to the platform and least prominent on the top. Huang and Lan [12] applied dynamic FEA to the design of a specific component, followed by reverse compensation to achieve greater dimensional accuracy in the part printed using SLA. Curl distortion of the bottom surface was identified as a major contributor to the inaccuracy of SLA prototypes. Lee et al. [13] used a neural network model to predict with reasonable accuracy the effects of the input parameters on the dimensional accuracy of the parts created. They found that layer thickness, hatch spacing and hatch over-cure were the most influential variables. Guangshen et al. [14] investigated the effects of four build parameters, namely the laser beam's scanning speed, cured line width compensation, hatch spacing and the coefficient of the resin's shrinkage compensation, on the dimensional accuracy of high-resolution SLA-printed parts. They concluded that the hatching space, the coefficient of the resin's shrinkage compensation and the interaction between the scanning speed and hatch spacing had the most significant effect on the dimensional accuracy of the parts tested. Cheng et al. [15] proposed that the selection of the correct orientation improved the accuracy of the parts produced using SLA. Six

sources of errors that were affected by the part's orientation during the building process were identified: tessellation, missing feature, over-cure, distortion and shrinkage, the container effect and the staircase effect. Zhou et al. [16] used the Taguchi method to determine the relationship between the quality of the parts printed using SLA and the variables involved in the input process. Their results pinpointed the optimal settings for the variables of layer thickness, resultant over-cure, hatch space, blade gap and part location. Jayanthi et al. [17] applied a one-way analysis of variance (ANOVA) to investigate the effects of different process parameters, for example, layer thickness, hatch spacing, fill cure depth and hatch over-cure, on the curl distortion in parts printed using SLA. They concluded that the four main parameters and their interactions contributed around 95% of the variation in curl.

1.2 Powder binder printing

PBP was developed in 1993 at the Massachusetts Institute of Technology [18]. In this process, layers are created by the selective distribution of binder liquid through an inkjet printer head over a flat layer of anhydrite powder in the x-y plane. Similar to SLA, the layers are formed on a piston-held platform that is lowered after the completion of each layer. After the completion of a layer, additional powder is distributed over the powder bed and a roller is then used to spread it evenly. Post-process treatments are commonly used to improve the finished surface and strength of the part.

Relvas et al. [19] compared the dimensional and geometric performance of four rapid prototyping processes: SLA, PBP, SLS, and FDM. PBP recorded the worst dimensional performance of all the RP processes, although the geometrical performance of PBP compared favourably with that of most of the other processes. Dimetriov et al. [20]

fabricated numerous test parts for measurement in order to determine which variables influenced the dimensional and geometric accuracy of the PBP process. They concluded that both types of accuracy were influenced by three major factors: powder material, build orientation and the magnitude of nominal dimension. Ollison and Berisso [21] conducted a series of experiments to determine the build variables that influenced the cylindricity of parts printed using PBP and found that only the build orientation had a statistically significant effect on the cylindricity of the parts. Hsu et al. [22] applied the Taguchi method to optimise the quality and efficiency of the build considering four process variables: layer thickness, the binder saturation level of the shell, and the core and location in the powder bed. Islam et al. [23] investigated the length, width, height and hole diameter of parts produced using PBP and found that the dimensions in the x-y plane were undersized, while those on the z-axis were about three to four times higher than the average error. Islam et al. [24] analysed the dimensional errors and repeatability of commonly used engineering parts, including a metric bolt, a gear and a shaft, produced using the PBP process. In most cases, the dimensional errors on the produced parts were within acceptable limits. However, the process was unsuitable for features that required very high dimensional accuracy and a good surface finish. Islam and Sacks [25] analysed the dimensional and geometric accuracy of various test parts. Their results showed the existence of a bottom surface concave curvature (inverse to the traditional curl). This curvature influenced the height error, which consisted of both a constant component and a cumulative error component.

A review of the available literature revealed a substantial body of work focussing on the analysis and optimisation of the dimensional accuracy of the SLA process. The phenomenon of ‘curl’ and the shrinkage that occurs in SLA printed parts are well

documented. However, the influence of the curl produced by volumetric shrinkage on the dimensional accuracy of the created parts has not yet been adequately investigated. Furthermore, only a limited number of studies have been carried out on the dimensional accuracy of PBP. Recently, Islam and Sacks [25] reported that the dimensional accuracy of PBP was affected by the volumetric expansion of powder material during setting in the presence of a water-based binder. The opposing nature of the volumetric changes that occur in these two RP processes (i.e. contraction in SLA and expansion in PBP) suggests that the dimensional accuracy of printed parts will be influenced in different ways. The objective of this research is hence to investigate this hypothesis in greater detail. This paper presents a comparative experimental investigation of the dimensional accuracy of the two RP processes—SLA and PBP—with a focus on the volumetric changes and their influence on the dimensional accuracy of the produced parts. This quantitative analysis will provide useful information on the accuracy of these two RP processes, which is vital for making an informed decision regarding the selection of the appropriate method for the design and manufacture of products.

2. Experimental work

The part used for this study, which was taken from [25], is displayed in Figure 1. It consists of six concentric cylinders with reducing diameters that are located on top of one another. A central hole of uniform diameter runs through the entire part. The base diameter, the maximum height and the central hole diameter are 126, 60 and 30 mm, respectively. This particular geometry was chosen because of its isosymmetric characteristics. Corner junctions were avoided because they could complicate the distortion patterns because of uneven volume changes in the x-y plane. The part was designed such that numerous dimensional measurements can be taken for each replicate,

thus reducing the number of replicates required for testing. Six different height measurements, six different external diameter measurements and the diameter of the central hole can be determined from a single replicate.

Four replicates of the test part were produced using a Z450 3D printer (Z Corporation, USA). The specifications of the Z450 3D printer are available in [26]. The printer has a specific resolution of 300 dpi×450 dpi, and the build size is 203 mm×254 mm×203 mm. The printer enables the selection of a build-layer thickness between 0.089 and 0.102 mm. The thickness selected for this experiment was the default setting of 0.102 mm. The time of printing was about 3h. The material used for the fabrication of the part was high-performance composite powder Z150 (calcium sulphate hemihydrate, or plaster of Paris) with a water-based clear binder solution zb63 (2-pyrrolidone). Each part was printed individually to avoid location errors in the powder bed.

A ProJet 3500 HDMax printer was used to produce four additional replicates of the test part. The specifications of ProJet 3500 HDMax printer are available in [27].The replicates were printed using the ultra-high definition (UHD) mode setting, which has a specific resolution of 750 dpi×750 dpi×890 dpi, a build volume of 298 mm×185 mm×203 mm and a layer thickness of 29 microns. The time of printing was about 15h. The material used for the fabrication of the part was UV-curable plastic VisiJet M3X. The support material was made from the white melt-away wax material, VisiJet S300. After the completion of each print, the part was subjected to post-processing, in which it was transferred to a thermal oven set at a constant 75 °C until all the wax used in the build process was removed. Any residual wax was then removed using a paper hand towel. The part was then set on a clean paper hand towel on a wooden bench to cool at ambient temperature.

Each completed part was transferred to a general-purpose coordinate measuring machine (CMM) (Discovery model D-8, Sheffield, UK), which collected measurement data through the selective probing of predetermined locations. The CMM has a position resolution of 0.1 microns. The axial repeatability of the measurement within its full travel area is ±2.5 microns. A spherical probe 4 mm in diameter (Renishaw Electrical Ltd., UK) was used. Measurements were taken of the central hole diameter, the outer diameters of each cylinder, the height of the each step and the base geometry. The probe locations used to take these measurements are shown in Figure 2. The base of the part was considered as the primary datum, which was placed on the flat granite table of the CMM. All measurements of height in the z direction were taken from the granite table. The surface topography of the datum surface was obtained by placing the part upside down on a fixture. The aligning capability of the CMM was used to align the datum surface with the CMM granite table. The diameters of the central hole and the outer cylinders were determined using the standard built-in software package for the CMM. Eight points at different angular locations in the same horizontal plane were probed. The diameter of the central hole was checked at height intervals of 1 mm, and the external diameter of each cylinder was checked at three height positions.

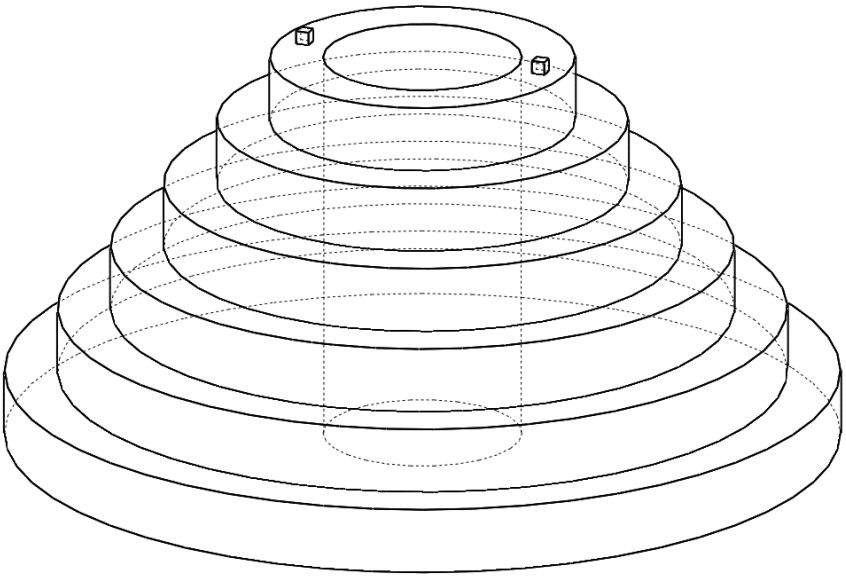

Figure 1: 3D sketch of test part [25]

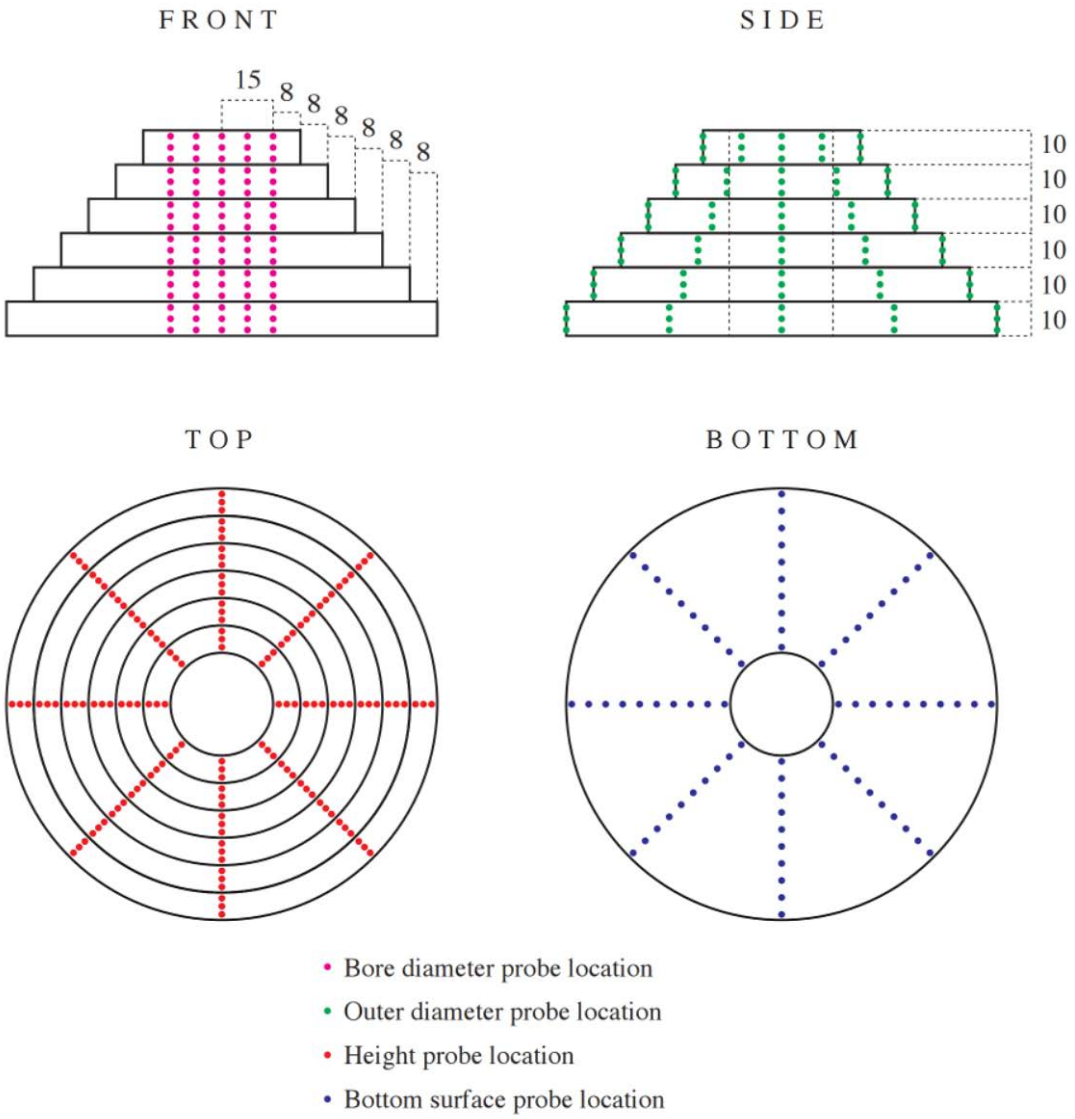

Figure 2: Probe touch locations (all measurements in millimetres) [25]

3. Results

3.1 Datum surface error

Figure 3 displays the datum surface error for each replicate produced using SLA and PBP. In SLA, the datum surface error varied between 0.427 and 0.439 mm with an average value of 0.434 mm and a standard deviation of 0.005 mm. In PBP, it varied between 0.187 and 0.353 mm with an average value of 0.258 mm and a standard

deviation of 0.072 mm. It should be noted that SLA produced an average datum surface error that was 68% greater than PBP, whereas the standard deviation was 14.4 times less than PBP.

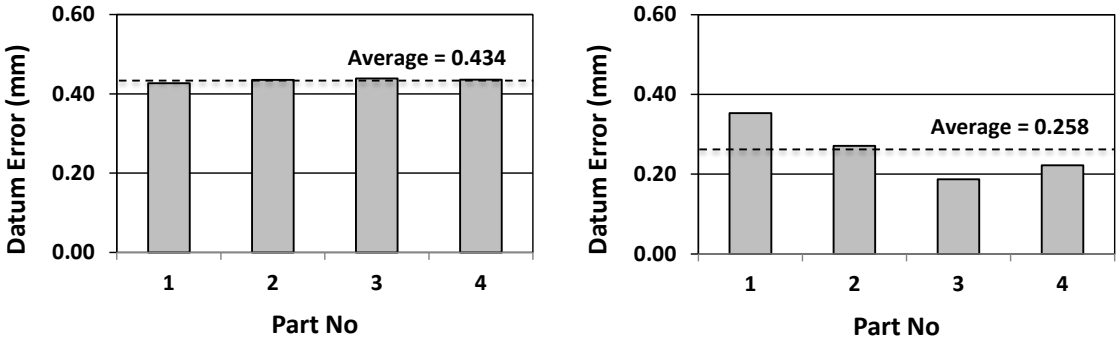

Figure 3: Datum surface error: (a) SLA and (b) PBP

The close inspection of the datum surfaces revealed that SLA produced a convex curvature, whereas PBP produced a concave curvature. Figure 4 presents an accentuated comparison of datum surface curvature produced by SLA and PBP. The surface topography of the datum surfaces for SLA and PBP are depicted in Figure 5. The average measurements of the datum surface with ± 3σ variations for SLA and PBP are shown in Figure 6. In SLA, the height from the lowest point increased with the increase in distance from the hole axis, producing the highest point at the periphery, whereas in PBP, the height from the lowest point decreased, producing the lowest point at the periphery. In both cases, the variations increased with the increase in distance from the hole axis, but in PBP, the variations were noticeably higher.

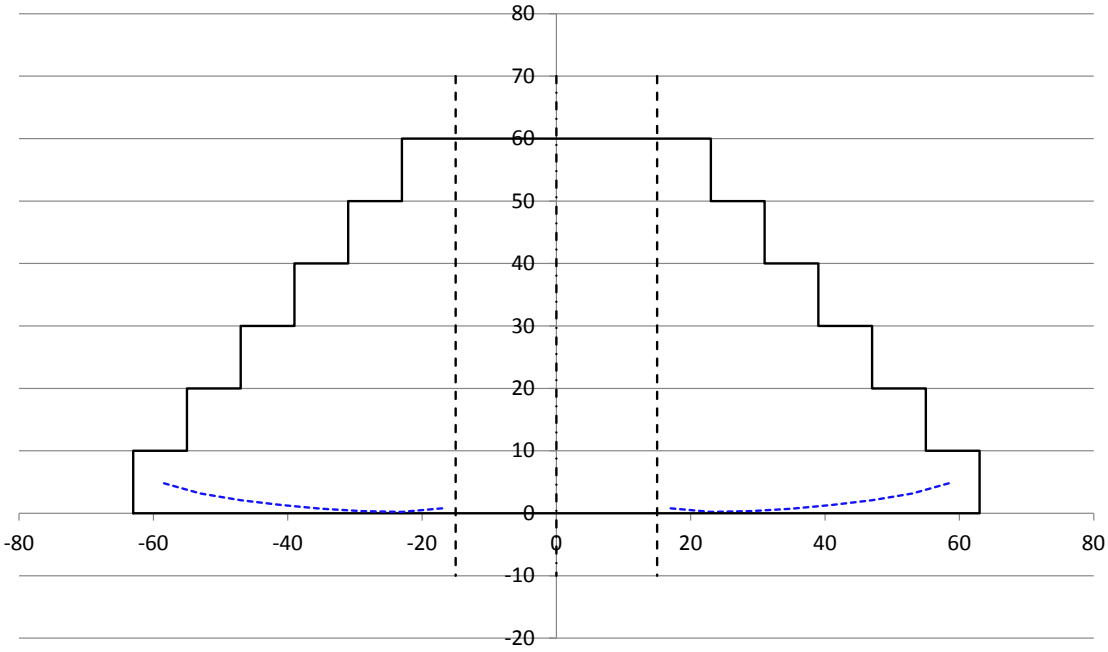

(a)

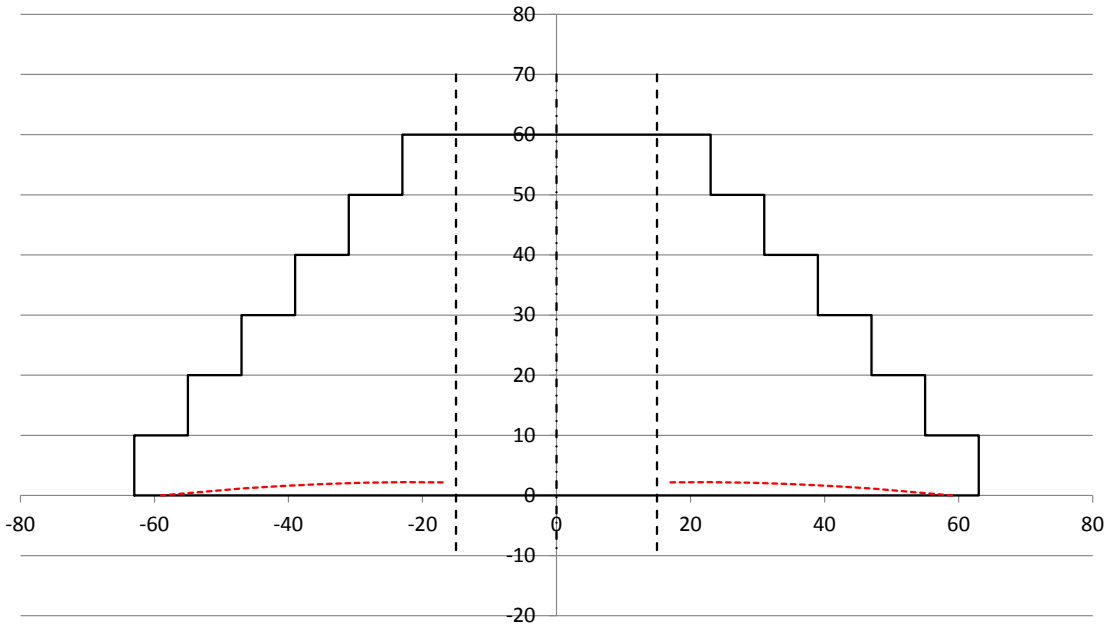

(b)

Figure 4: Accentuated comparison of datum surface curvature: (a) SLA and (b) PBP

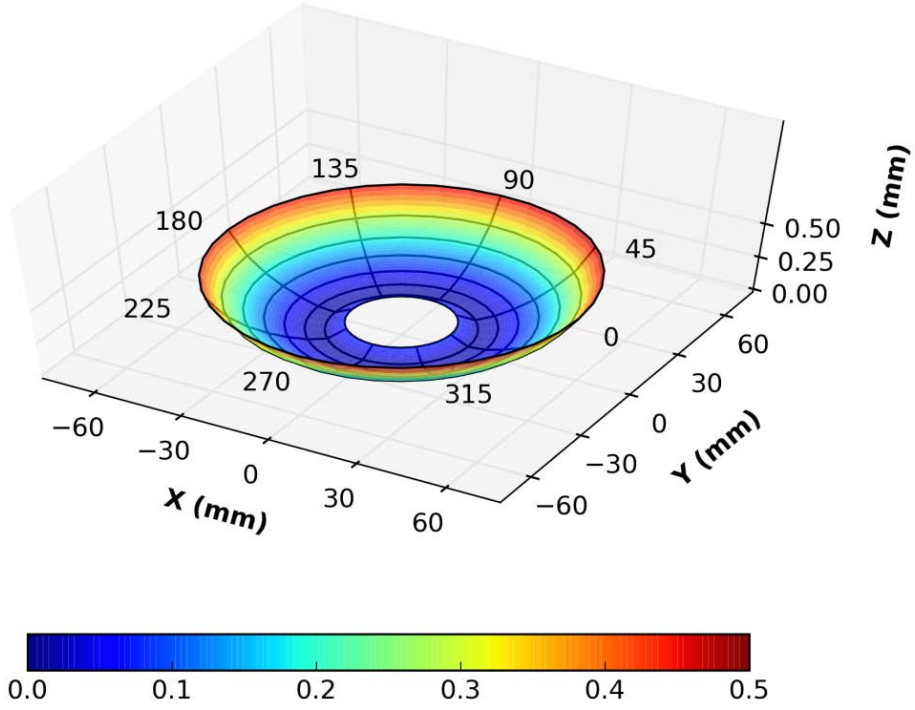

(a)

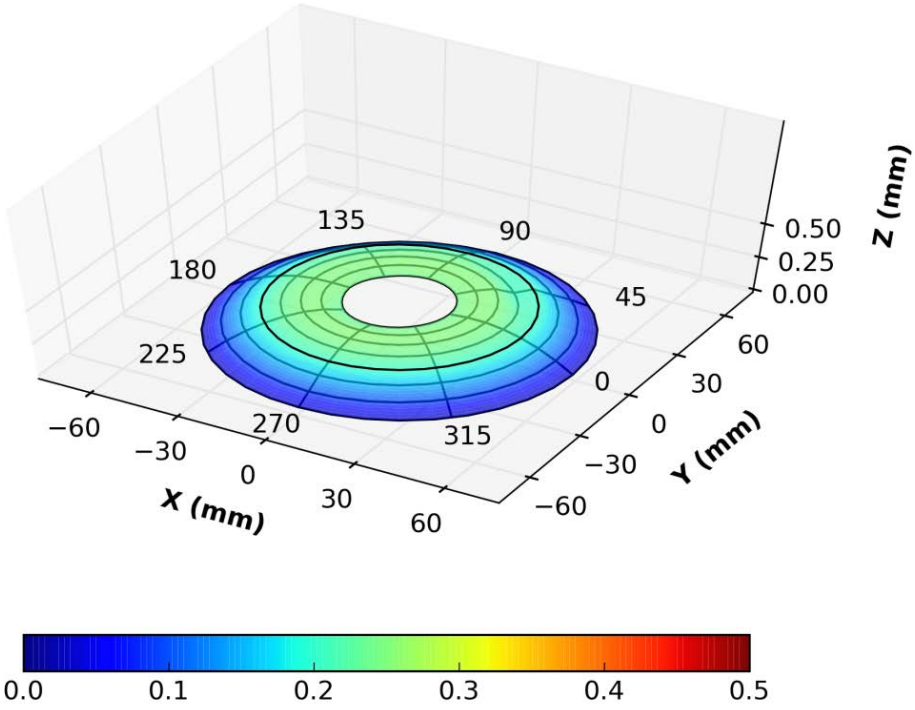

(b)

Figure 5: Surface topography of datum surfaces: (a) SLA and (b) PBP

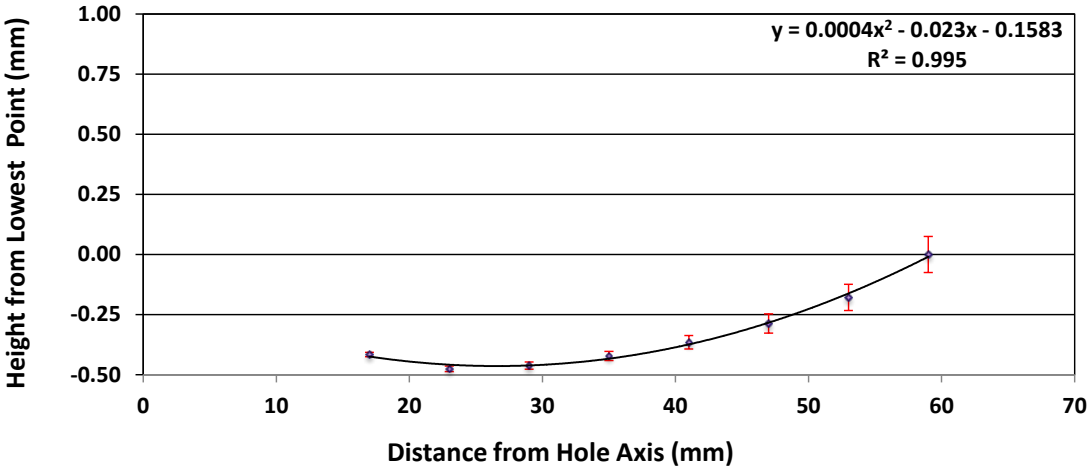

(a)

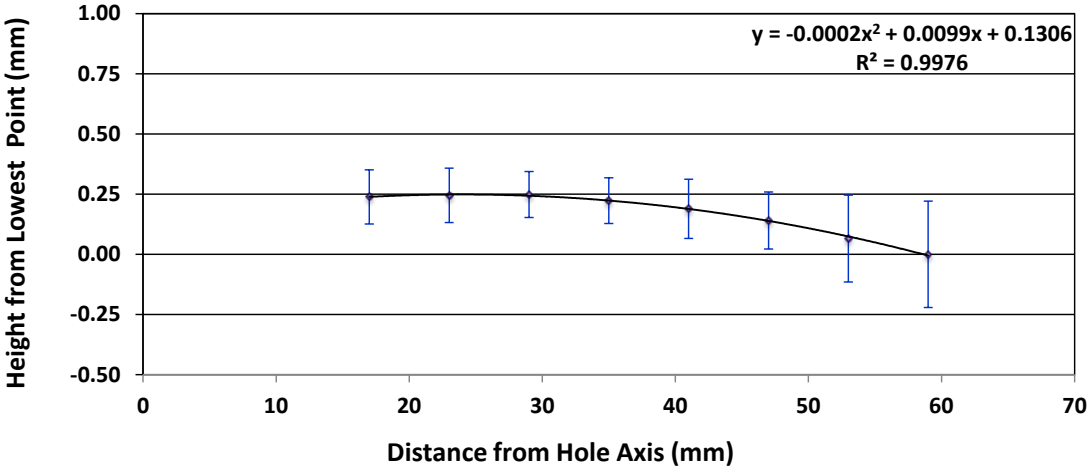

(b)

Figure 6: Datum surface measurement results: (a) SLA and (b) PBP

3.2 Z-axis error

Figure 7 displays the average errors for the total height (60 mm) for each replicate produced by SLA and PBP. In SLA, it varied between -0.014 and 0.002 mm, with an average value of -0.005 mm and a standard deviation of 0.007 mm. In PBP, it varied

between 0.765 and 1.150 mm, with an average value of 0.954 mm and a standard deviation of 0.157 mm. It should be noted that PBP produced an average height error that was 190 times larger than that in SLA, and the standard deviation in PBP was 22 times higher than in SLA.

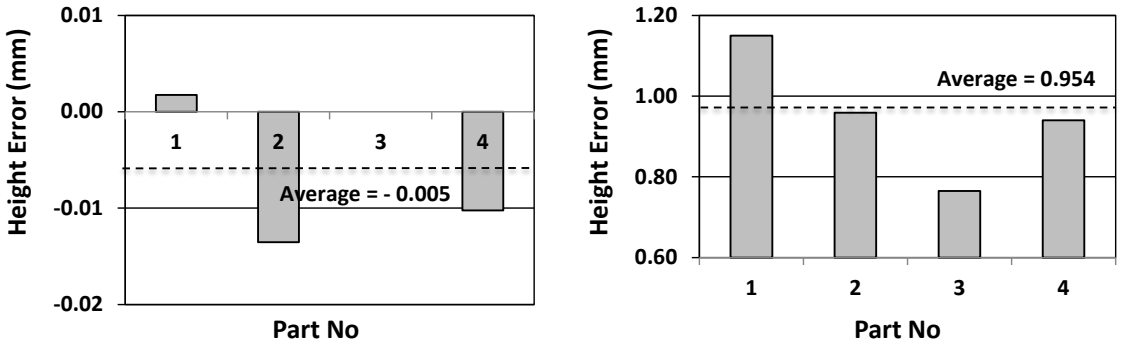

(a) (b)

Figure 7: Height error: (a) SLA and (b) PBP

Figure 8 shows the change in average height error with the nominal heights of SLA and PBP and their respective trend lines. In SLA, the trend line was a quadratic function, and the height error decreased with the increase in nominal height. The variations also decreased with the increase in nominal height. In PBP, the relationship was linear, and the height error increased with the increase in nominal height. The variations were similar as the nominal height increased. Figure 9 shows an accentuated comparison of the height errors produced by SLA and PBP.

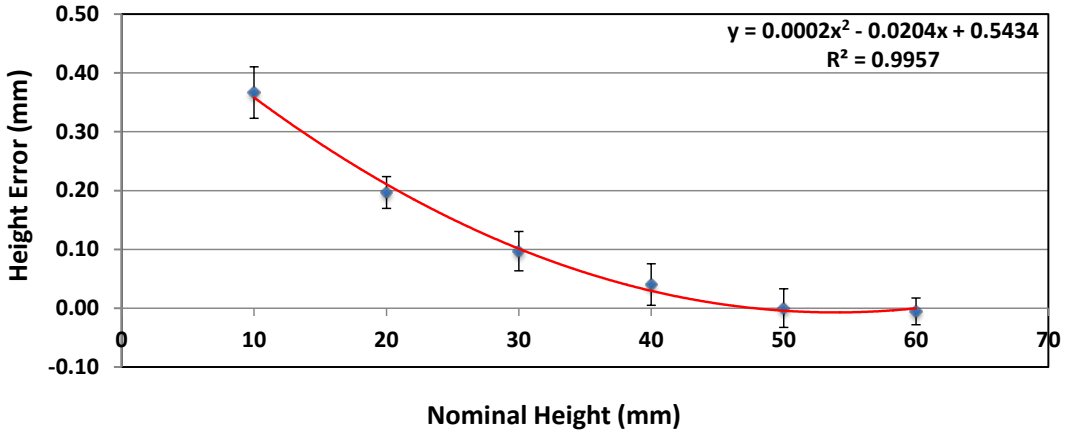

(a)

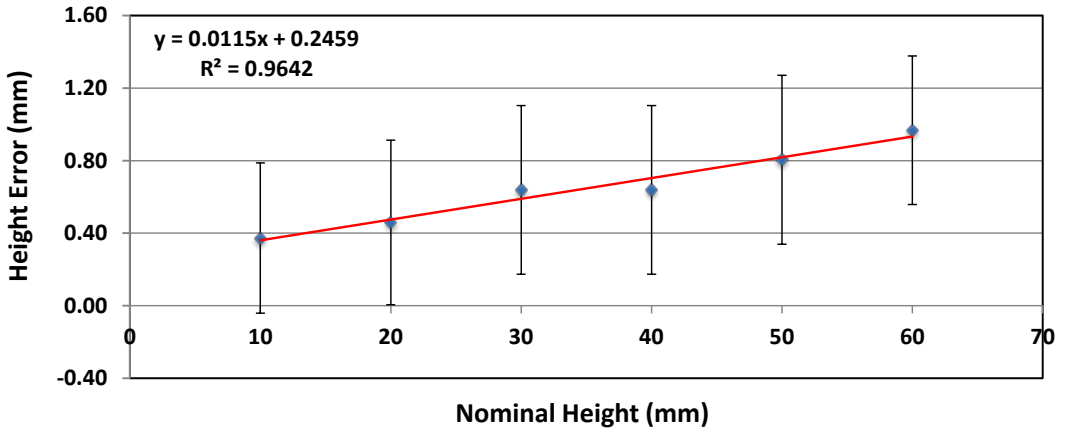

(b)

Figure 8: Change in height error with nominal height: (a) SLA and (b) PBP

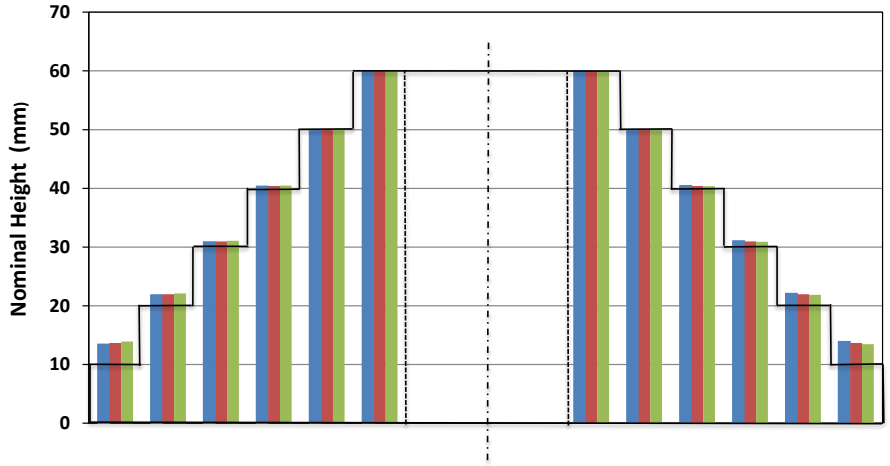

(a)

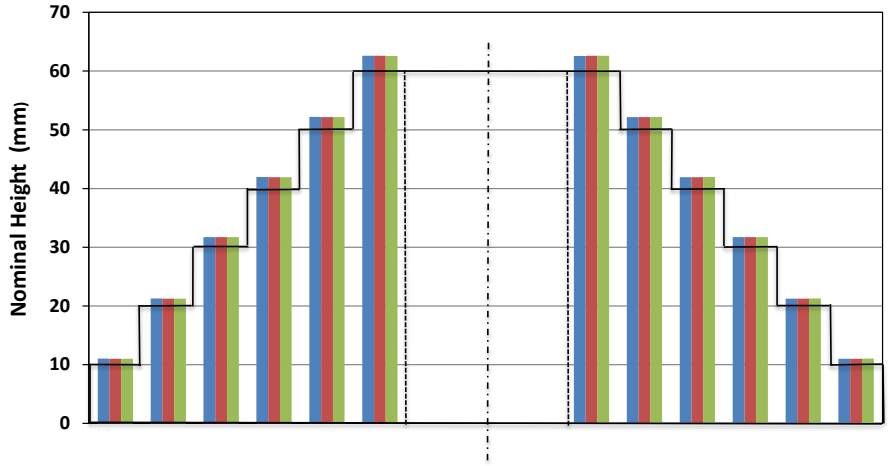

(b)

Figure 9: Accentuated representation of height error: (a) SLA and (b) PBP

3.3 X-y plane error

Figure 10 shows the errors in central hole diameter in SLA and PBP. In SLA, the error ranged between -0.150 and -0.132 mm with an average value of -0.141 mm and a standard deviation of 0.008 mm. In PBP, it varied between -0.059 and -0.012 mm with an average value of -0.031 mm and a standard deviation of 0.020 mm. It should be

noted that SLA produced an average error in hole diameter that was about 4.5 times larger than in PBP. However, the standard deviation was 2.5 times less than in PBP.

Figure 11 shows an accentuated plot of the deviation from the nominal values of the central vertical hole in the test parts. The measurements of both PBP and SLA showed diameters smaller than the nominal values. The SLA dimensions were smaller than PBP dimensions.

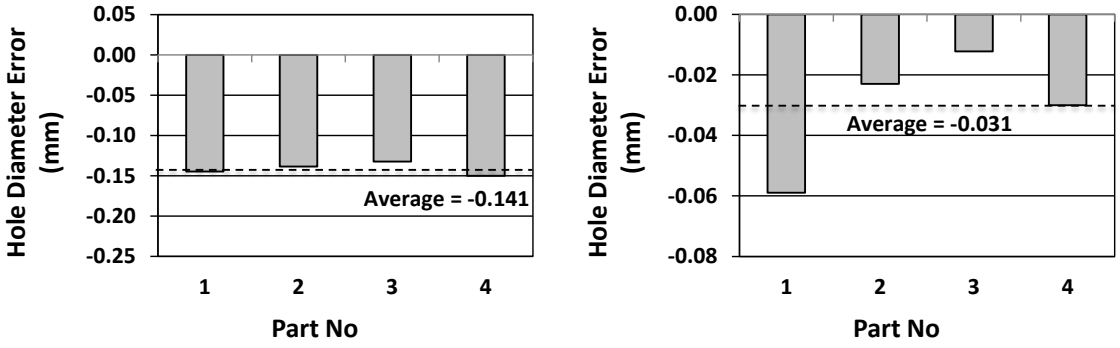

(a) (b)

Figure 10: Hole diameter error: (a) SLA and (b) PBP

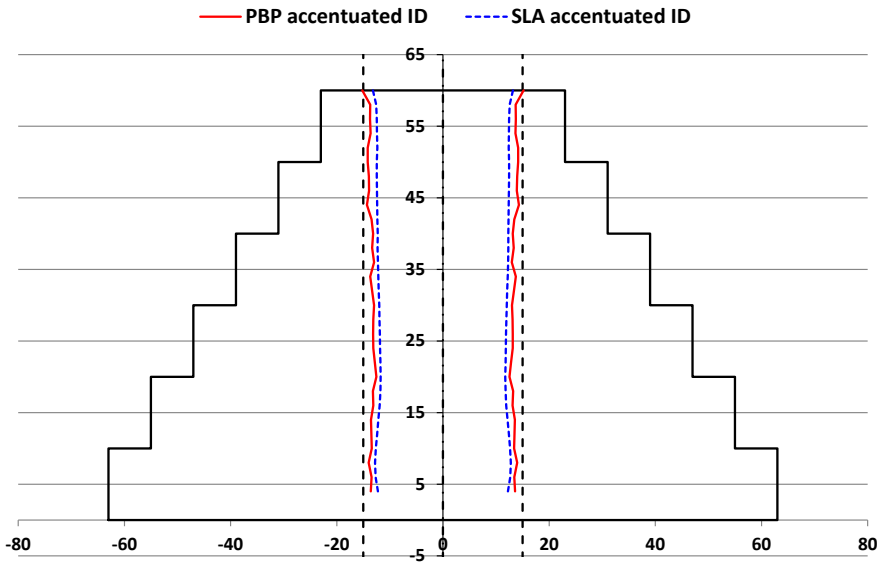

Figure 11: Accentuated hole diameter comparison

Figure 12 shows the errors in the outer diameters in SLA and PBP. In SLA, the error varied between -0.612 and -0.592 mm with an average value of -0.606 mm and a standard deviation of 0.009 mm. In PBP, it varied between -0.058 and -0.025 mm with an average value of -0.045 mm and a standard deviation of 0.014 mm. It should be noted that SLA produced an average outer diameter error that was about 13.5 times larger than the PBP; however, the standard deviation was about 1.5 times less than the PBP.

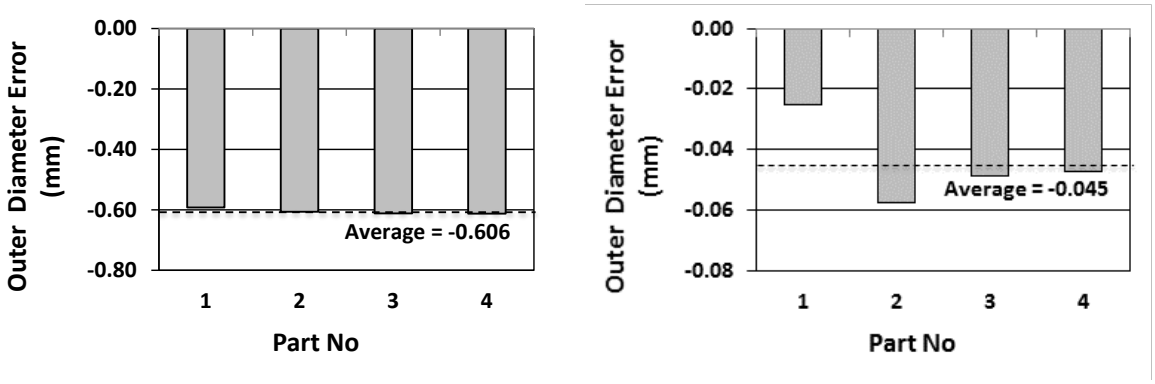

(a) (b)

Figure 12: Outer diameter error: (a) SLA and (b) PBP

Figure 13 shows the change in outer diameter error with the nominal diameters of SLA and PBP and their respective trend lines. In SLA, the diameter error was greatly influenced by the change in nominal diameter. The trend line was a linear function and the diameter error increased with the increase in the nominal diameter. The variations were very small. In PBP, although the change in diameter error was very small, the variations were high. Figure 14 presents an accentuated comparison of the outer diameters produced by SLA and PBP.

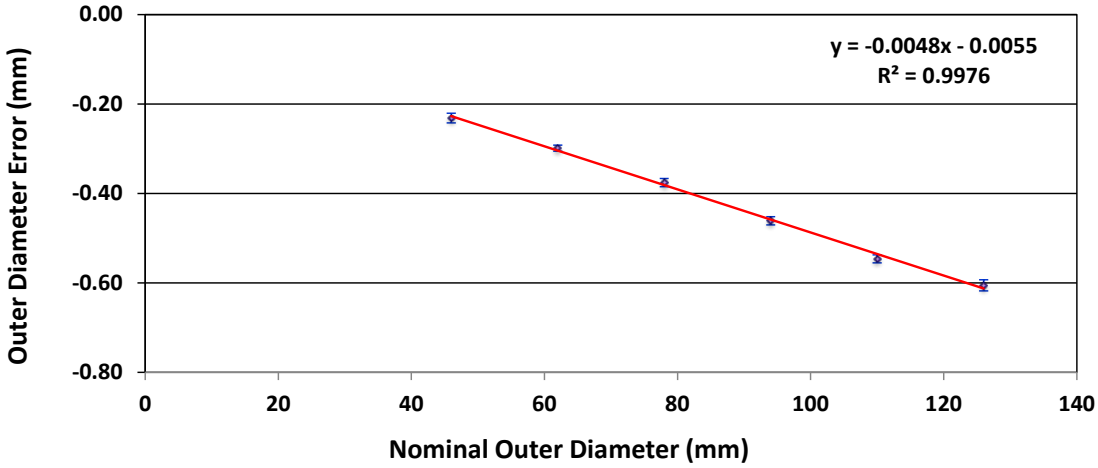

(a)

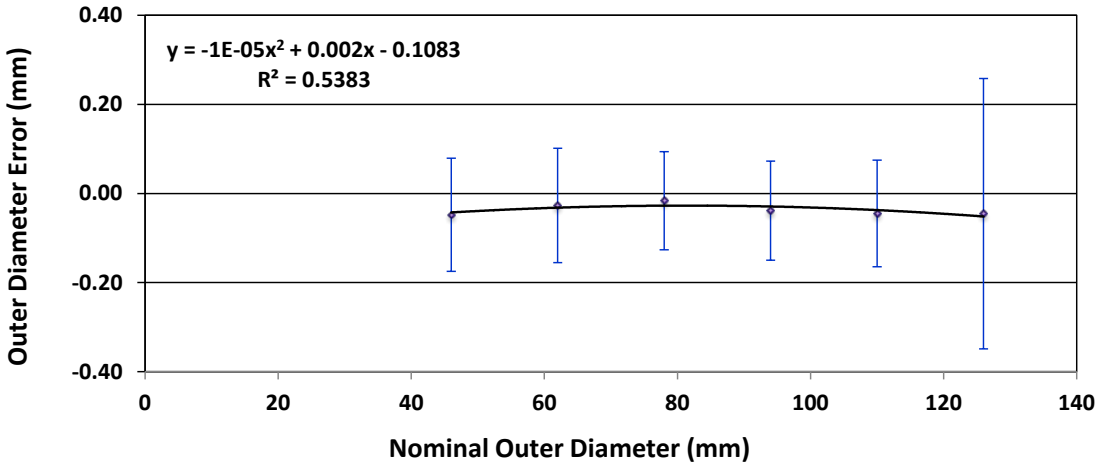

(b)

Figure 13: Variations in outer diameter with nominal diameter: (a) SLA and (b) PBP

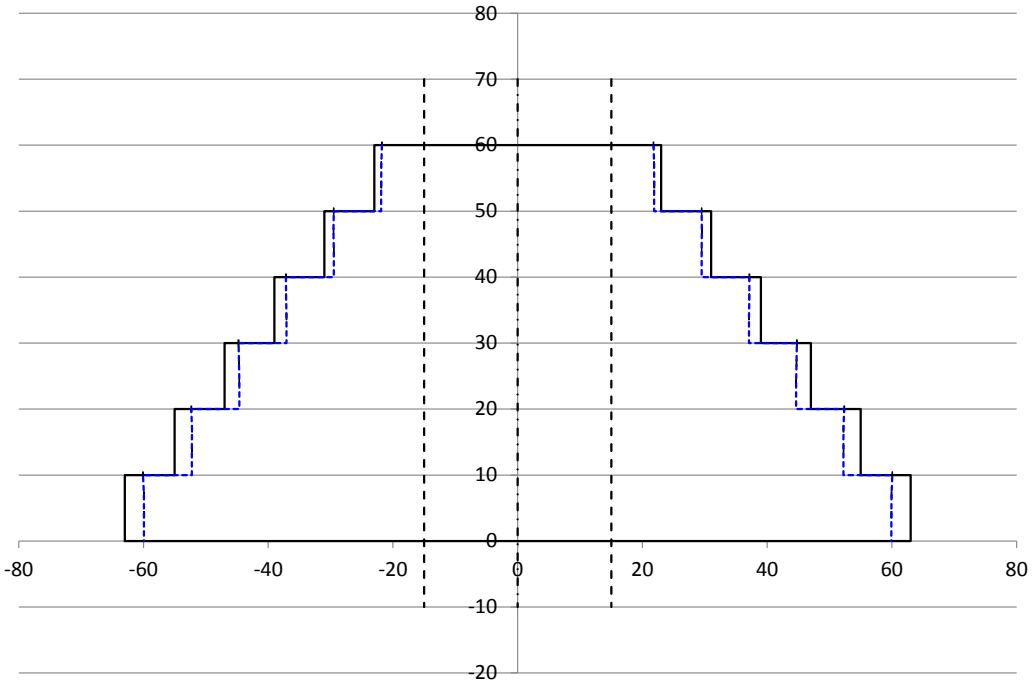

(a)

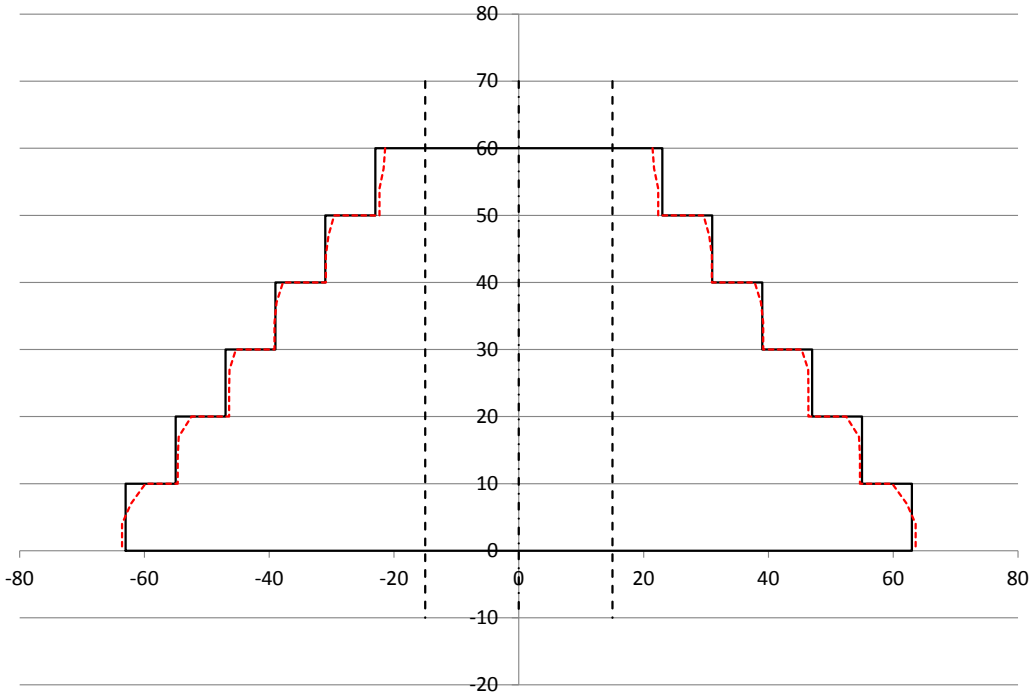

(b)

Figure 14: Accentuated outer diameter comparison: (a) SLA and (b) PBP

4. Analysis and discussion

The error analysis of both RP processes found that the inherent changes in volume caused the variations in dimension. In SLA, volumetric contraction was found to occur during the photo-polymerisation process, resulting in a convex datum. A similar trend was reported in the literature [12]. In PBP, however, volumetric expansion was found to occur because of the hygroscopic expansion of the plaster of Paris (the powdered material used in PBP) when it set in the presence of water-based binder, which resulted in a concave datum. A similar trend has been observed in Islam and Sacks [25].

Although the SLA process yielded higher dimensional accuracy and repeatability in the z direction than the PBP process, its average datum surface error was greater by 68%. The reason for the greater datum error in SLA is difficult to explain because two entirely different processes were employed. However, one reason may be that the layer thickness used in SLA (29 microns) was far smaller than that used in PBP (102 microns), which caused greater curling after the volumetric changes in SLA. Further research is needed to test this hypothesis. Nevertheless, the large datum error in SLA is worrisome. Because all dimensions refer to it, the dimensional accuracy of any part is significantly influenced by the accuracy of the datum surface.

This study established that in SLA, the height error improved with the increase in nominal height, whereas it deteriorates in PBP (Figures 8 and 9). The reason is that the height error comprises two components: constant error and cumulative error [25]. Because of volumetric contraction, the layer thickness produced in SLA was smaller than the design thickness was. Consequently, the constant error on the datum surface was compensated because of the increased number of layers. The layer thickness

produced in PBP was larger than the design thickness because pf volumetric expansion. Consequently, because of the increased number of layers, additional error components were added to the constant datum surface error. In this study, the total height (60 mm) produced by SLA was highly accurate and undersized by only 5 microns. However, it was expected that further increases in height, the total height of the part would be increasingly undersized.

Consistent with Islam and Sacks [25], the findings of the present study confirm their assertion that both a constant error and a cumulative component of the z-direction error existed in the PBP parts. In addition, the constant error could be attributed to the datum surface error, and the cumulative error was caused by overall volumetric expansion. It is worth noting that the y-intercept of the height error trend line (0.2459 mm) shown in Figure 8b is very close to the average datum surface error (0.258 mm) shown in Figure 3b. A different trend was observed in the SLA parts. Figure 8a shows that when the height error in the nominal values was plotted against the nominal values for the SLA parts, the resultant plot had a high correlation with a positive quadratic function in which the gradient was negative. The y-intercept of the height error trend line (0.5434 mm) shown in Figure 8a was close to the average datum surface error (0.434 mm) shown in Figure 3a. Thus, it can be concluded that SLA parts also had a constant error caused by the curvature on the bottom surface. Unlike the PBP parts, however, the SLA data resembled a function that at all times had a negative gradient and the gradient was not constant but instead had a negative rate of change.

An analysis of the x-y plane error was conducted to achieve a complete picture of the nature of deformation in these RP processes. In both cases, the internal diameter was smaller than nominal values, as shown in Figure 10. The negative deviation was greater

in the SLA parts than in the PBP parts. Moreover, the SLA parts showed less data spread and more consistent errors than the PBP showed.

The external diameter measurements of the PBP parts showed no obvious trend. When the deviations from nominal outer diameters were plotted against their nominal values, the SLA parts presented a high correlation with a negative linear function (Figure 13a). This negative gradient was consistent with the volumetric shrinkage that occurred in the SLA process.

The precision of a manufacturing process is often expressed by the international tolerance (IT) grade [28]. The smaller the grade of the IT number, the higher the precision of the process. The following formula [29-31], which is based on the tolerance standards for cylindrical fits, was used to calculate the IT grade in which process capability tolerance was replaced by six times the standard deviation of measured dimension data.

$$PC = \left(0.45\sqrt[3]{X} + 0.001X\right) 10^{\frac{IT-16}{5}} \quad (1)$$

where PC is the process capability tolerance (mm), X is the manufactured dimension (mm) and IT is the IT grade number.

Table 1 presents the comparison of the dimensional error results for SLA and PBP. The calculated IT grade values showed that the SLA was far more precise than the PBP was. In SLA, the IT grade varied between 6.108 and 10.769, with an average value of 8.049. In PBP, the IT grade varied between 10.396 and 15.637, with an average value of 13.054. In terms of dimensional accuracy, SLA was better in the z direction, whereas PBP produced better dimensional accuracy in the x-y plane.

Table 1: Comparison of dimensional errors

		SLA					PBP				
Input parameters	Unit	Height	Height	Hole Dia	Outer Dia	Outer Dia	Height	Height	Hole Dia	Outer Dia	Outer Dia
Design size	mm	10	60	30	46	126	10	60	30	46	126
Measured mean size	mm	10.367	59.995	29.859	45.768	125.394	10.373	60.954	29.969	45.952	125.955
Dimensional error	μm	367	-5	-141	-232	-606	373	954	-31	-48	-45
6 x standard deviation	μm	88	45	54	21	25	828	819	108	255	606
IT grade		10.769	7.967	8.890	6.513	6.108	15.637	14.267	10.396	11.937	13.031

5. Conclusion

This study conducted a comparative analysis of the dimensional errors in the RP processes using SLA and PBP. The findings of the volumetric changes in each RP process were consistent with previous studies. The results of this study provide new insights into the nature of the dimensional errors in these processes, which were caused by two contrasting volumetric changes. The major findings of this study are listed below:

- The precision of SLA was far better than PBP.
- The dimensional accuracy SLA was better in the z direction, whereas PBP produced better dimensional accuracy in the x-y plane.
- In both RP processes, the height error was comprised of two components: constant error and cumulative error. The constant error component was equal to the datum surface error.
- Within the considered range, the height error in SLA improved with the increase in nominal height, whereas it deteriorated in PBP.

References

1. Wohler T, Gornet T. History of Additive Manufacturing, Wohlers Report, http://wohlersassociates.com/history2014.pdf, (accessed on 25/1/2016).
2. Kruth J-P, Leu MC, Nakagawa T. Progress in Additive Manufacturing and Rapid Prototyping. CIRP Annals - Manufacturing Technology. 1998;47(2). Epub 540.
3. Gibson, I, Rosen, DW, Stucker, B. Additive manufacturing technologies. Chapter 4, Photopolymerization Processes, New York: Springer, 2010.
4. Noorani, R. (2006). Rapid prototyping: principles and applications. John Wiley & Sons Incorporated.
5. Yan X, Gu P. A review of rapid prototyping technologies and systems. Computer-Aided Design. 1996;28(4):307-318.
6. Freed WS, Hull CW, Lewis CW, Smalley DR, Spence ST, Vinson WB. Stereolithographic curl reduction. Google Patents; 1989.
7. Fadel, G. M., & Kirschman, C. (1996). Accuracy issues in CAD to RP translations. Rapid Prototyping Journal, 2(2), 4-17.
8. Bjørke, Ø. (1991). How to make stereolithography into a practical tool for tool production. CIRP Annals-Manufacturing Technology, 40(1), 175-177.

9. Narahara H, Tanaka F, Kishinami T, Igarashi S, Saito K. Reaction heat effects on initial linear shrinkage and deformation in stereolithography. Rapid Prototyping Journal. 1999;5(3):120-8.
10. Salmoria GV, Ahrens CH, Beal VE, Pires ATN, Soldi V. Evaluation of post-curing and laser manufacturing parameters on the properties of SOMOS 7110 photosensitive resin used in stereolithography. Materials & Design. 2009;30(3):758-63.
11. Huang, Y. M., & Lan, H. Y. (2006). Compensation of distortion in the bottom exposure of stereolithography process. The International Journal of Advanced Manufacturing Technology, 27(11-12), 1101-1112.
12. Huang YM, Lan HY (2005) Dynamic reverse compensation to increase the accuracy of the rapid prototyping system. Journal of materials processing technology, 167(2), 167-176.
13. Lee SH, Park WS, Cho HS, Zhang W, Leu MC (2001) A neural network approach to the modelling and analysis of stereolithography processes. Proceedings of the Institution of Mechanical Engineers, Part B: Journal of Engineering Manufacture, 215(12), 1719-1733..
14. Guangshen, X., Jing, J., Sheng, L., Ronghua, Q., & Huan, P. (2009, April). Research on optimizing build parameters for stereolithography technology. In Measuring Technology and Mechatronics Automation, 2009. ICMTMA'09. International Conference on (Vol. 2, pp. 883-886). IEEE.
15. Cheng W, Fuh JYH, Nee AYC, Wong YS, Loh HT, Miyazawa T. Multi-objective optimization of part-building orientation in stereolithography. Rapid Prototyping Journal. 1995;1(4):12-23.
16. Zhou JG, Herscovici D, Chen CC (2000) Parametric process optimization to improve the accuracy of rapid prototyped stereolithography parts. International Journal of Machine Tools and Manufacture, 40(3), 363-379.
17. Jayanthi S, Keefe M, Gargiulo EP (1994, August) Studies in stereolithography: influence of process parameters on curl distortion in photopolymer models. In Solid Freeform Fabrication Symposium 1994 (pp. 250-258). University of Texas, Austin.
18. Printing of the Paper, MITnews, http://newsoffice.mit.edu/2011/3d-printing-0914, September 14, 2011, (accessed on 25/1/2016)
19. Relvas C, Ramos A, Completo A, Simões JA (2012) A systematic approach for an accuracy level using rapid prototyping technologies. Proceedings of the Institution of Mechanical Engineers, Part B: Journal of Engineering Manufacture, 226(12), 2023-2034.
20. Dimitrov D, Van Wijck W, Schreve K, De Beer N (2006) Investigating the achievable accuracy of three dimensional printing. Rapid Prototyping Journal, 12(1), 42-52.
21. Ollison T, Berisso K (2010) Three-dimensional printing build variables that impact cylindricity. J. Ind. Technol, 26(1), 2-10.
22. Hsu TJ, Lai WH (2010) Manufacturing parts optimization in the three-dimensional printing process by the Taguchi method. Journal of the Chinese Institute of Engineers, 33(1), 121-130.
23. Islam, M. N., Boswell, B., & Pramanik, A. (2014, April). Dimensional Accuracy Achievable by Three-Dimensional Printing. In IAENG Transactions on Engineering Sciences: Special Issue of the International MultiConference of Engineers and Computer Scientists 2013 and World Congress on Engineering 2013 (p. 263). CRC Press
24. Islam, M. N., Pramanik, A., & Slamka, S. (2016). Errors in different geometric aspects of common engineering parts during rapid prototyping using a Z Corp 3D printer. Progress in Additive Manufacturing, 1-9. DOI 10.1007/s40964-016-0006-7
25. Islam, M. N., & Sacks, S. (2016). An experimental investigation into the dimensional error of powder-binder three-dimensional printing. The International Journal of Advanced Manufacturing Technology, 82(5-8), 1371-1380.
26. Presenting the ZPrinter 450, http://www.zcorp.com/documents/105_Z%20Corp%20ZPrinter%20450%20Intro.pdf (accessed on 25/1/2016).
27. Projet 3500 SD&HD Professional Printers, http://au.3dsystems.com/sites/www.3dsystems.com/files/projet_3500_plastic_0115_usen_web.pdf (accessed on 25/1/2016).
28. Islam, M. N. (1995, November). A CMM-based geometric accuracy study of CNC end milling operations. In Proceedings of sixth international conference on manufacturing engineering (pp. 835-841).
29. Conway, H. G. (1966). Engineering tolerances: a study of tolerances, limits and fits for engineering purposes, with full tables of all recognized and published tolerance systems. Pitman.

30. Farmer, L. E. (1999). Dimensioning and tolerancing for function and economic manufacture. Blueprint Publications, Sydney.
31. Bjørke Ø (1989). Computer-Aided tolerancing, ASME, New York.